PHYSICAL REVIEW B VOLUME 35, NUMBER 18 15 JUNE 1987-II

LO-phonon oscillations and electron freeze-out in transport through In-InP and Sn-InP contacts

Pong-Fei Lu* and D. C. Tsui
Department of Electrical Engineering, Princeton University, Princeton, New Jersey 08544

H. M. Cox
Bell Communications Research, Murray Hill, New Jersey 07974

(Received 8 August 1986)

An investigation of electrical transport through In and Sn contacts to high-purity InP is reported. At 4.2 K, the *I-V* characteristics show a gap at small *V*, within which no current flows through the contacts, and oscillations at higher *V* in the reverse bias, corresponding to electron injection into InP. Large-amplitude oscillations, ~50% the background differential conductance, and as many as 32 periods have been observed; their *T* and *B* dependences have been measured. The conductance gap, observable to ~10 K, is due to electron freeze-out and the oscillations, observable to above 78 K in dI/dV, are due to emission of LO phonons in InP. At present, there is no theoretical understanding of these experimental observations. Only a qualitative discussion of the data is given using a point-contact model. The LO-phonon oscillations in this model result from a modulation in the current injection via a voltage feedback mechanism, which is consistent with measurements also made on n^+-i-n^+ structures.

I. INTRODUCTION

Recently,[1] we reported the observation of an oscillatory conductance in electrical transport through $\mathrm{In}_x\mathrm{Ga}_{1-x}\mathrm{As}$ contacts, which corresponded to a series of dips in the *I-V* characteristics in both bias polarities. Similar conductance oscillations in the reverse bias, corresponding to electron injection into the semiconductor, were first reported in Au-InSb tunnel junctions by Katayama and by Komatsubura and Cavenett,[3] and more recently in tunneling into GaAs through a $\mathrm{Al}_x\mathrm{Ga}_{1-x}\mathrm{As}$ barrier by Hickmott *et al.*[4] and by Eaves *et al.*[5] All these experiments had two features in common: (1) the host semiconductors were high-purity materials, and (2) the period was approximately equal to the longitudinal-optical (LO) phonon energy, $\hbar\omega_0$, of the high-purity semiconductor. Although it was recognized very early that the oscillatory phenomenon had to result from emission of LO phonons by the hot electrons injected through the junction, how such emission processes could cause the observed oscillations were never understood. Only very recently, after the experiment of Hickmott *et al.*, have appreciable theoretical efforts been made towards a fundamental understanding of this unexpected electronic phenomenon.[6-10]

In this paper, we want to report a systematic study of electrical transport through In and Sn metal contacts to high-purity InP crystals. These contacts show rectifying *I-V* characteristics, which cannot be associated with either a diffusion barrier, or tunneling through a planar Schottky barrier. Two striking features are observed in the *I-V* characteristics. First, for $T \lesssim 10$ K, a gap exists around zero bias, within which there is virtually no current flow through the contact. This conductance gap is due to electron freeze-out in InP and it increases, as expected, in the presence of a strong magnetic field *B*. Second, strong LO-phonon oscillations are observed in *I-V* in the reverse bias, corresponding to electron injection into InP. The oscillations are observable at 78 K in the dI/dV versus *V* data and their amplitude, at 4.2 K, amounts to an ~50% change in the average dI/dV. These results are unique in that the LO-phonon oscillations and the electron freeze-out are observable and studied in the same experiment. The fact that the oscillations persist to at least 78 K, far above the temperature (~10 K) at which the conductance gap vanishes, is evidence that electron freeze-out is not essential to the observation of the conductance oscillations.

At the present, there is no theoretical understanding of these striking experimental observations. Only a qualitative discussion of the results is given using a model[11] for the point contact between a metal and a semiconductor. Within this model, the oscillations are attributed to modulation of the bias across the contact by relaxation of the injected hot electrons via LO-phonon emission. It is a voltage feedback mechanism inherent to injection of hot carriers into an electrode made of a low-carrier-density material. This explanation is substantiated by data from samples with a n^+-i-n^+ structure [i.e., a high-purity InP layer sandwiched by two heavily doped InP layers]. Their *I-V* characteristics show the conductance gap due to electron freeze-out, but not the conductance oscillations.

This paper is organized as follows. In Sec. II, we describe the experiment and present the data. The results are discussed in Sec. III using the model of Vengurlekar and Inkson.[11] Some concluding remarks are given in Sec. IV.

II. EXPERIMENTS

Our samples are high-purity *n*-type epitaxial InP layers, ~4 μm thick, grown by trichloride-vapor levitation epitaxy[12] on the (100) surface of heavily doped InP substrates. The epilayers are unintentionally doped, with a residual carrier density ranging from 6×10^{14} to 2×10^{15} cm^{-3}. The crystals are first slightly etched to remove the surface layer, then metal dots, $\sim0.25\times0.25$ mm^2,[2] are made by thermal evaporation of a thick (In,Sn) film in a vacuum of $\sim1\times10^{-6}$ Torr. Ohmic contacts to the high-purity InP are made through the n^+-type InP substrate by soldering with In. Finally, the samples are heated in H_2 atmosphere at 350 °C for 90 sec to facilitate the observation of the LO-phonon oscillations. This point will be clarified later on when we examine the data. The measurements are two-terminal I-V measurements and standard modulation techniques are used to obtain the derivatives dI/dV and d^2I/dV^2. Some of the data are also obtained using a computer-aided data-acquisition system and the derivatives from digital differentiation. The temperature variation is achieved with a Heli-tran system, and a closed-cycle refrigerator.

Figures 1 and 2 are examples of the I-V characteristic of typical Sn and In contacts from room temperature (RT) to 4.2 K. The bias voltage is that of the metal electrode with respect to the n^+-type InP substrate. We see that the contacts are slightly non-Ohmic at RT, and are rectifying at $T \lesssim 78$ K. Since these two metal contacts show similar behavior in all our measurements, we will concentrate on the data of Sn-InP contact from now on. Figure 3 is an enlarged version of Fig. 1 at 4.2 K for $-0.5 < V < 0.05$, which shows two striking features. First, there is a flat region around zero bias, within which there is virtually no current flow. Second, for $V<0$, corresponding to electron injection into the InP, a series of oscillations are superimposed on the rather linear background. These two features are more clearly seen in the dI/dV-V data shown in Fig. 4, where the flat region is manifested as a "gap." The oscillations, with a period ($\sim$43.7 mV) approximating the LO-phonon energy of InP,[13] 43 meV, are identified as a series of dips in the dI/dV at $e\,|V|\sim n\hbar\omega_0$, where $n=1,2,3,\ldots$. They are already observable at 77 K, and at 4.2 K, the amplitude amounts to as high as a 50% change of the mean dI/dV at low biases. The oscillations persist to the highest bias applied across the structure. This fact is illustrated in

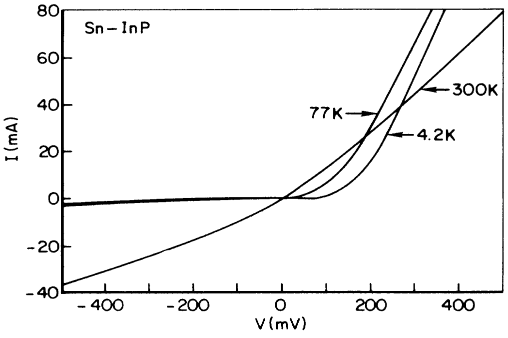

FIG. 1 I-V characteristics of a Sn-InP contact at 300, 78, and 4.2 K.

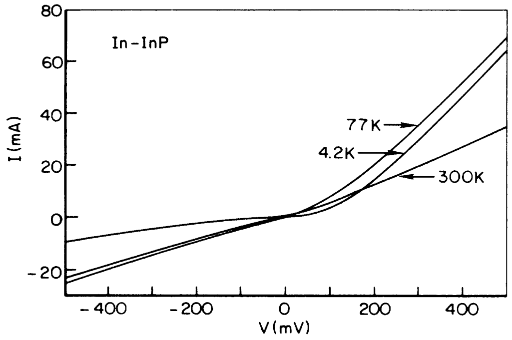

FIG. 2. I-V characteristics of an In-InP contact at 300, 78, and 4.2 K.

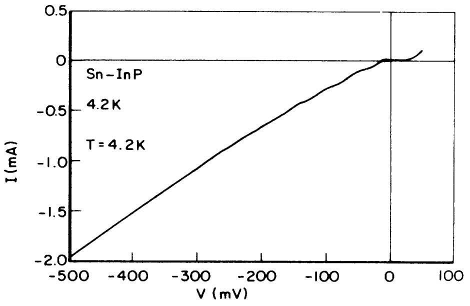

FIG. 3. I-V characteristics of a Sn-InP contact for $-0.5 \lesssim V < 0.05$ V at 4.2 K.

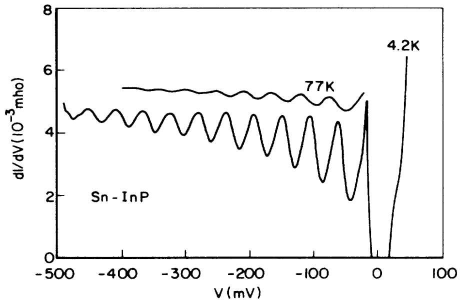

FIG. 4. dI/dV-V of the Sn-InP contact of Fig. 4 at 78 and at 4.2 K.

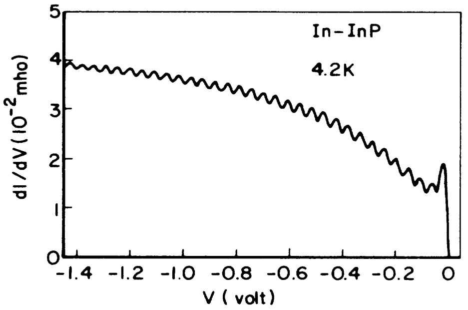

FIG. 5. dI/dV-V of an In-InP contact for V up to 1.4 V in the reverse bias, corresponding to electron injection into the InP.

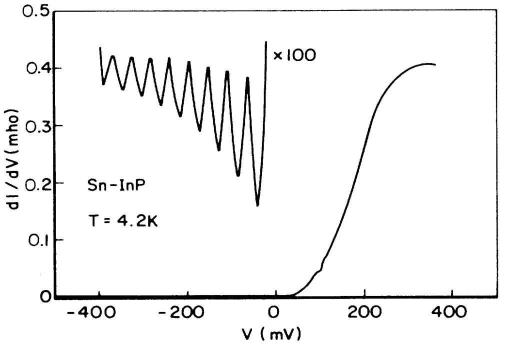

FIG. 6. dI/dV-V of a Sn-InP contact for $-0.5<V<0.5$ V at 4.2 K.

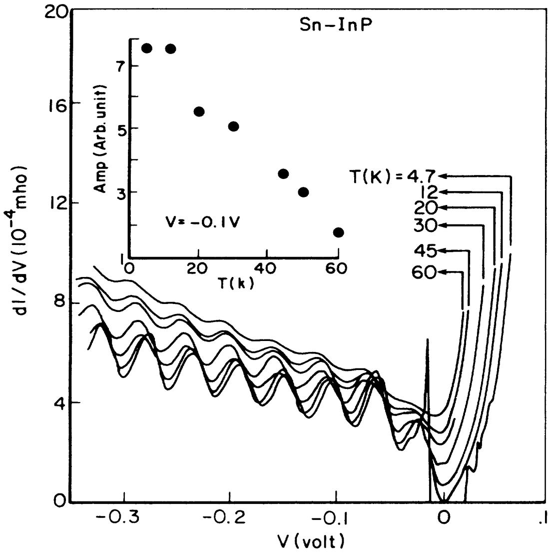

FIG. 8. T dependence of dI/dV-V of a Sn-InP contact. Inset shows the dependence of the LO-phonon oscillation amplitude on T at $V=-0.1$ V.

Fig. 5, where 32 periods can be seen for $-1.4<V<0$ V, with only a slight decrease in amplitude at high biases (the sample is the same In-InP contact whose I-V characteristic is shown in Fig. 2).

In Fig. 6 we show the dI/dV-V at 4.2 K for $-0.5<V<0.5$ V. The asymmetry in the two bias polarities is obvious, and we see that, at $|V|\sim 0.4$ V, the ratio of dI/dV in the two bias polarities is about 100. We should note that, within our experimental resolution, the oscillations are not seen in the forward bias even when the second derivative is taken. This is in contrast to the results for the In-In$_x$Ga$_{1-x}$As contacts reported earlier,[1] where oscillations are seen in both polarities.

These data are taken from contacts heated in H_2 atmosphere at 350 °C for 90 sec. Before this annealing, the I-V characteristic is also rectifying, but the resistance in the reverse bias is too high to allow dI/dV measurements. Thus, the annealing step is necessary for the observation of the oscillations in these samples. In some other samples, the contact resistance prior to annealing is sufficiently low for derivative measurements, yet annealing is still needed to enhance the oscillatory structures. Figure 7 shows an example of this. We see that before annealing

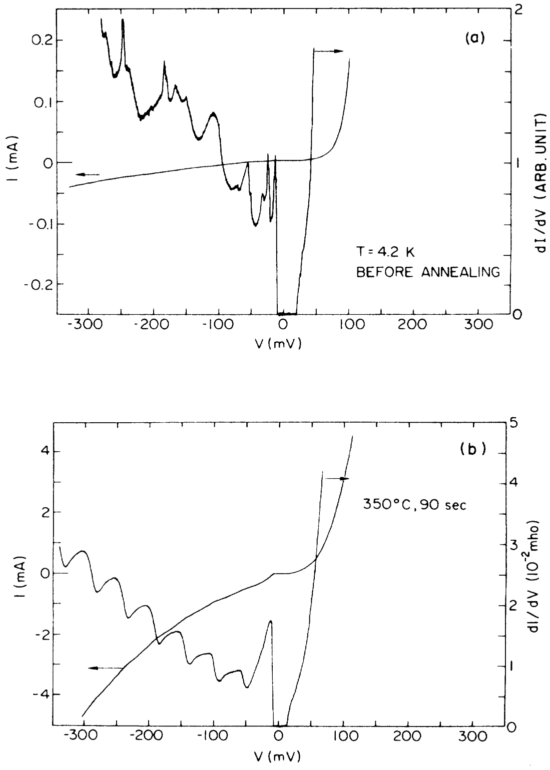

FIG. 7. I-V and dI/dV-V characteristics of an In-InP contact (a) before annealing (in H_2 atmosphere at 350 °C for 90 sec), and (b) after annealing.

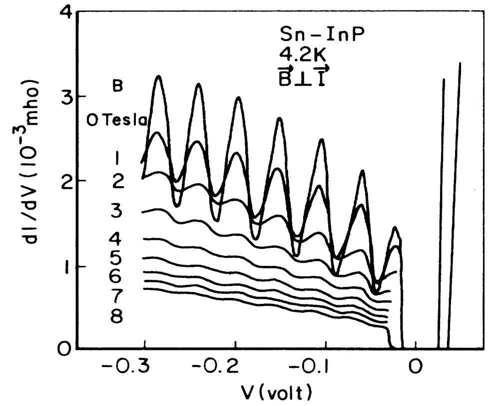

FIG. 9. dI/dV-V of a Sn-InP contact as a function of a perpendicular magnetic field ($\mathbf{B}\perp\mathbf{I}$) at 4.2 K.

[Fig. 7(a)], there are unidentified spikes in the dI/dV, which make it difficult to identify the oscillations. These spikes are reproducible from measurement to measurement for the same contact, and are not spurious noise. After annealing, the spikes disappear and clean periodic structures are apparent; meanwhile, the current level increases approximately ten times. Although these observations are generally true for all the samples we have studied, annealing is not always necessary and its use is determined on a sample-to-sample basis.

We studied the temperature dependences and found that the oscillation amplitude decreases with increasing T for T above ~10 K (Fig. 8), but it remains virtually constant when T is lowered from 4.2 K to 1.5 K. At the same time, the dips in dI/dV shift toward higher energies with the period remaining unchanged. This shift was also observed by Cavenett[3] on InSb samples, and its origin is not identified yet. We have not observed sharpening of the line shape, when T is lowered from 4.2 to 1.5 K, as reported by other workers.[2,5] It is worth noting that in Fig. 8 the voltage gap disappears at ~12 K, while the oscillatory structures persist to much higher temperatures.

When a parallel magnetic field $\mathbf{B}||\mathbf{I}$, is applied, there is no observable effect on either the period or the amplitude of the oscillations. On the other hand, in the presence of a $\mathbf{B}\perp\mathbf{I}$, the oscillations decrease in amplitude as shown in Fig. 9, but they remain discernible at $B=80$ kG. These results are consistent with earlier observations on the $\mathrm{In}_x\mathrm{Ga}_{1-x}\mathrm{As}$ contacts.[1] Also, the voltage gap increases in a strong B (Fig. 10). A faster increase is seen for $\mathbf{B}\perp\mathbf{I}$ than for $\mathbf{B}||\mathbf{I}$.

III. DISCUSSIONS

A. Rectifying *I-V*

The rectifying characteristics of Sn and In contacts on InP cannot be associated with a diffusion barrier, as evident from the top panel of Fig. 11, which shows a semilog plot for the forward I-V in Fig. 2. According to the ideal thermionic emission model, the $\log I$ versus V, for $V > 3kT/e$, should be a straight line with a slope equal to $e/\eta kT$, where η is the ideality factor; the intercept at $V=0$ can be used to derive the barrier height ϕ_b if the Richardson constant is known.[14] Here, $\log I$ has a nonlinear dependence on V, suggesting that the data cannot be associated with a diffusion barrier. We also measured the current at fixed bias voltage as a function of T from $T=8$ to 300 K. The bottom panel of Fig. 11 shows the data for $V=20$ mV, where $\log_{10}(I/T^2)$ is plotted against $1/T$. While the thermionic emission model predicts a straight line with a slope equal to $-e\phi_b/k$, our data show positive slopes everywhere, except for a small region around $T \sim 50$ K. Moreover, for $V \gtrsim 200$ mV, the current at 300 K is less than that at 77 and 4.2 K. These results indicate that the transport cannot be due to thermal diffusion over a surface barrier.

Next, we recall that there has recently been considerable interest in the metallurgical interaction at the InP-metal interface. Both In and Sn are known to form low electron potential barriers,[15,16] or even Ohmic contacts[16] to n-type InP(110). Brillson and Brucker[17] have pointed out that interface reaction can cause metals to diffuse into the semiconductors and form electrically active sites. These sites may change the local work function of the materials

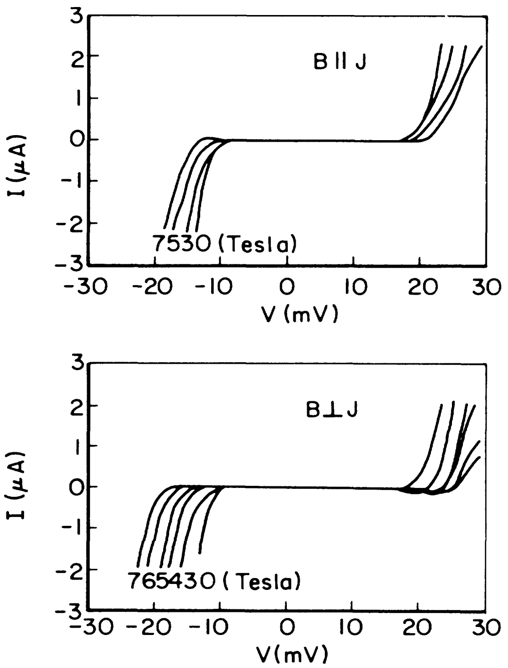

FIG. 10. I-V characteristics of a Sn-InP contact at 4.2 K in the presence of perpendicular magnetic field ($\mathbf{B}\perp\mathbf{I}$) and parallel magnetic fields ($\mathbf{B}||\mathbf{I}$).

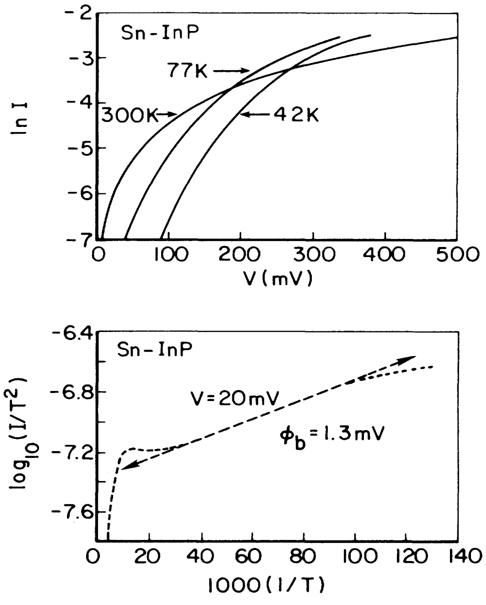

FIG. 11. Top panel: $\log I$ vs V of a Sn-InP contact at 300, 78, and 4.2 K. Bottom panel: $\log(I/T^2)$ vs $1/T$ of the same Sn-InP contact at $V=20$ mV.

and the local doping density at the interface. Consequently, the resulting metal-semiconductor (M-S) contacts may fall into the category of point contacts. Williams *et al.*[18] have shown, by the photoemission measurement, that the etched InP surface has a large band-gap oxide, which is consistent with In_2O_3. They also found that Sn films deposited at room temperature formed islands or clusters.[16] The point contact can be envisaged as follows. The actual M-S contact is through a large number of tiny spots or channels, which may result from the porous native oxide (i.e., there are small areas of free InP surface not covered by the oxide where direct contacts with the metal take place). Otherwise, the clustering of the deposited metal can also make the contact pointlike rather than planar. The atomic interdiffusion can drastically change the properties of the semiconductor surface in the vicinity of the contact. Two possibilities arise. (1) The increase in surface doping concentration makes electron tunneling[19] possible. These "point" tunnel junctions differ from the planar tunnel junctions in that they do not have the translational symmetry parallel to the planar surface, therefore the transverse momentum is not a conserved quantity in the tunneling process. (2) The local work function of the semiconductor surface changes in such a way that an accumulation layer of electrons exists at the M-S interface, which forms low-resistance current paths. In either case, the current flow is through these tiny spots or channels.

Point-contact spectroscopy[20] has long been used in metals to study the electron-phonon interaction. Its application to M-S contacts was first reported by Pepper[21] on the Al—n^+-Si contacts. They observed various structures in the d^2I/dV^2-V characteristic due to electron-phonon interactions. Subsequently, Vengurlekar and Inkson[12] proposed a theoretical model which we adopt to discuss our data.

Their model is illustrated in Fig. 12. They assumed, for convenience, a semispherical metal tip with a radius $r=b$. The contact region extends to $r=d$ and the semiconductor electrode is from $r=d$ to $r=R$. In the absence of inelastic collisions, the applied V drops entirely in the contact and there is no depletion region in the semiconductor.

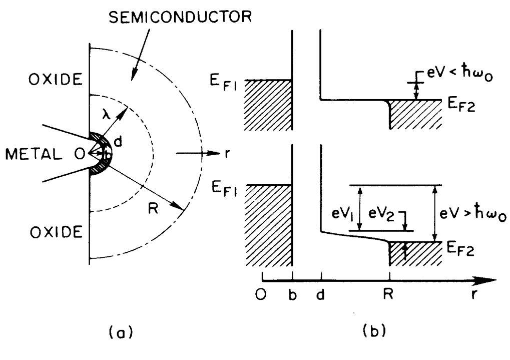

(a) (b)

FIG. 12. The geometry and the energy diagrams illustrating the point-contact model of Vengurlekar and Inkson (Ref. 12).

The electrons, injected through the contact into the bulk semiconductor, are hot with an excess energy above E_F. They will subsequently relax the excess energy by phonon emissions. The total current at any position r is considered to consist of two components: the current due to the hot electrons which have not relaxed their excess energy, and the current due to the bulk electrons. At $r=d$, the current has its contribution only from the injected hot electrons. As these injected electrons move into the bulk, they lose their kinetic energy and thus are slowed down by phonon emissions. In order to satisfy current continuity, the loss in the current contribution by these injected hot electrons, due to phonon emissions, is compensated by the bulk electrons in the semiconductor. This bulk current contribution results from the fact that, due to phonon emission by the injected electrons, the equilibrium distribution function is disturbed and an electric field builds up in the bulk semiconductor. Vengurlekar and Inkson[11] derived an expression for the I-V characteristic and showed that if $\lambda/d \gg 1$, where λ is the average inelastic scattering length, $I \sim G_0(V)V$ in the zeroth order, and $G_0(V)$ is usually a slowly varying function. We have seen in Fig. 4 that our experimental I-V characteristic in the negative bias, i.e., when the electrons are injected into the semiconductor, is fairly linear (except for the gap near zero bias), consistent with their model.

B. LO-phonon oscilations

Here, we give a qualitative discussion of the LO-phonon oscillations using the same model. We assume, for simplicity, that the LO-phonon emissions are the only scattering events in the semiconductor. In the case of a negative bias, electrons are injected into the semiconductor electrode, as illustrated in Fig. 12. When $eV < \hbar\omega_0$, phonon emission is not allowed and all the injected electrons can reach the back contact at $r=R$ without losing any kinetic energy. There is no current contribution from bulk electrons in the semiconductor and, consequently, no voltage drop in the electrode. The bias V_1 across the point contact, which controls the injection, is the entire applied voltage [i.e., $V_1 = V$, as in the top illustration of Fig. 12(b)]. As V increases, the current increases proportionally. When eV reaches the LO-phonon emission threshold, $\hbar\omega_0$, the injected electrons, with an excess kinetic energy equal to $\hbar\omega_0$, will rapidly relax their energy by emitting LO phonons. This energy loss by these injected electrons causes a decrease in the current carried by them. However, as mentioned above, the relaxation process perturbs the bulk electron distribution and causes a current contribution, J_b, from the bulk electrons to maintain current continuity. The electric field due to this current at r is $E(r)=J_v(r)/\sigma$, where σ is the electrical conductivity of the semiconductor and the voltage drop across the semiconductor electrode is $V_2 = \int_R^d E(r)dr$. As a result, V_1 is no longer equal to V, but $V_1 = V - V_2$, as illustrated in Fig. 12(b). In other words, as V approaches the phonon emission threshold, only part of the bias increment, δV, applied to the sample will appear as the bias increment across the contact, δV_1, which controls the current increment δI injected into the semiconductor.

Therefore, there will be a dip in dI/dV versus V at $eV \sim \hbar\omega_0$.

It should be emphasized that the total current is the integrated contribution from all the electrons that can be injected into the semiconductor electrode. When $eV \sim \hbar\omega_0$, only those electrons in the metal electrode at E_{F1} can emit LO phonons in the semiconductor. All other electrons will traverse the semiconductor and reach the back contact without any energy loss. As V keeps increasing above the phonon emission threshold, more and more electrons will be injected into the semiconductor with kinetic energies larger than $\hbar\omega_0$. Each of these electrons will rapidly emit an LO phonon and subsequently reach the back contact without further loss of energy. In other words, the current will again increase proportionally until $eV \sim 2\hbar\omega_0$, when the electrons injected from E_{F1} in the metal can relax their excess energy by sequentially emitting two phonons. The loss of these high-energy electrons again causes a sharp decrease in the bias increment δV_1 across the point contact and, consequently, another dip in dI/dV at $eV \sim 2\hbar\omega_0$. The same process recurs whenever eV is approximately equal to multiples of the LO-phonon energy, $\hbar\omega_0$, and it leads to a series of dips with a period of $\sim \hbar\omega_0$. In a real sample, scattering by impurities and acoustic phonons will smooth these dips into oscillations with a period $\Delta V \sim \hbar\omega_0/e$.

In this model, the LO-phonon oscillations result from a modulation of the bias across the contact, which controls the current injected into the semiconductor. The bias modulation is a consequence of the increase in the current component carried by the bulk electrons in the semiconductors. It is a voltage feedback mechanism inherent to hot-carrier injection into a low-carrier-density electrode. Therefore, the oscillations are to be observed only in high-purity materials in the reverse bias, corresponding to injection into the semiconductor.

The oscillation amplitude is expected to decrease at high temperatures due to the increasing acoustic phonon scattering, as was experimentally observed. In addition, electron-electron scattering can also relax the excess energy of the injected electrons and compete with the LO-phonon emission process. This competing energy relaxation mechanism also makes the LO-phonon oscillations more difficult to observe in high-electron-density samples. The magnetic field effects, as shown in Fig. 9, can be qualitatively understood as follows. The injected electrons are accelerated by a large electric field as they pass through the contact. This huge energy pickup will make the electronic motion highly directional along the current direction as they enter the bulk semiconductor. Therefore, a **B** parallel to **I** will not have any effect, whereas a perpendicular **B** is expected to smear out the oscillations due to the bending of the electron motion by the Lorentz force.

C. Conductance gap

We attribute the conductance gap (in Figs. 3 and 4) to electron freeze-out in the high-purity InP. At low T, all the electrons are frozen onto their parent donors and the InP, is, in effect, an insulator. For small V, virtually no current can flow through the structure. However, the electric field in the InP increases with increasing V. At sufficiently high V, the donors in InP can be ionized to give rise to the observed onset of current flow as shown in Fig. 3 and the well-defined conductance gap in Fig. 4. The gap is wider in V in the forward bias than in the reverse bias, reflecting the asymmetry of the device structure. Similar observation has been reported on InSb by Mansfield and Ahmasd.[22] Fenton and Haering[23] showed that there exists a critical carrier density n_0, beyond which the screening will prevent freeze-out at $\mathbf{B}=0$. For InP, we estimate n_0 to be $\sim 3\times10^{16}$ cm^3 using Eq. (18) of Ref. 23, and we observe no gap for samples with $n \geq 10^{17}$ cm^3. In the presence of a strong B, Yafet *et al.*[24] showed that the contraction of the electronic charge distribution in the plane perpendicular to **B** causes an increase in the ionization energy. This increase is seen as the gradual increase of the gap in Fig. 10. The gap is wider when $\mathbf{B}\perp\mathbf{I}$, as was observed earlier in InSb samples by Mansfield and Ahmasd.[22]

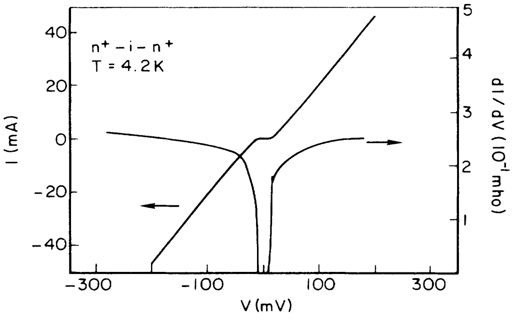

FIG. 13. I-V characteristics and dI/dV-V of an n^+-i-n^+ InP structure.

We also measured the I-V characteristics of several samples with n^+-i-n^+ structure, where an n^+-type InP layer ($\sim 2\ \mu$m, $n \geq 10^{18}$ cm^{-3}) is grown on top of the high-purity epilayer. In this case the Ohmic contacts to the high-purity InP are through the n^+-type InP from both sides. Figure 13 shows the I-V and the dI/dV-V characteristics of a typical sample at 4.2 K. We find no oscillations in the I-V characteristics and its derivatives. The conductance gap, on the other hand, is well defined and symmetric as expected. This result demonstrates that direct metal contact to the high-purity InP is crucial for the observation of oscillatory structures. Without the n^+-type InP top layer, the voltage drop occurs mostly in the metal-semiconductor contact region and a large electric field is created at the contact. Only a small portion of the voltage drop is in the bulk to maintain current continuity. On the other hand, in the n^+-i-n^+ structure, all the voltage drop occurs in the high-purity InP layer. The voltage feedback mechanism that we have discussed is inoperative and, consequently, no LO-phonon oscillations can be expected.

IV. CONCLUSIONS

In summary, an investigation of the electrical properties of In and Sn contacts to high-purity InP is reported. Two striking features are observed in the I-V characteristics: a gap at small V, within which no current flows through the contacts; and oscillations, due to LO-phonon emission, at higher biases in the reverse polarity, corresponding to electron injection into InP. A qualitative discussion of the results is given in terms of a model, due to Vengurlekar and Inkson[11] for metal-semiconductor point contacts. The conductance gap, observable to ~ 10 K, is due to electron freeze-out in InP. The oscillations are explained as coming from the emission of LO phonons in the high-purity InP by the injected "hot" electrons. They result from a modulation of the bias across the contact, which controls the current injection. The modulation arises from a voltage feedback mechanism inherent to hot-carrier injection into an electrode of a low carrier density. This model is consistent with T and B dependences of our data and also with our measurements made on n^+-i-n^+ InP structures.

Finally, it should be mentioned that several recent theoretical models explaining the oscillations observed in the experiments on $Al_xGa_{1-x}As$ tunnel junctions utilize a similar barrier-modulation mechanism. In these models, the barrier modulation, due to changes in the voltage drop in the high-purity GaAs, is caused by the changes in the space charge in GaAs. In Leburton's model,[8] the changes are created by the ionization of neutral donors by acoustic phonons, which in turn are created by the LO phonons emitted by the injected electrons. In the model by Taylor *et al.*,[10] they are due to impact ionization of the neutral donors by the injected hot electrons themselves as they approach the n^+-GaAs contact to the high-purity GaAs. Both models require the presence of neutral donors, i.e., electron freeze-out, in the GaAs electrode. The model of Hanna *et al.*[7] however, does not rely on electron freeze-out in GaAs. The changes in the space-charge result from a mechanism involving one-dimensional polarons. Ihm,[9,25] on the other hand, explains the oscillations in Hickmott's experiment as due to self-energy corrections from electron—LO-phonon interactions to the density of final states at an energy $\sim \hbar\omega_0$ above E_F in the n^+-GaAs substrate. In the discussion of our data, we have neglected both the space-charge effect and the density-of-states effect. We concentrated only on the feedback mechanism of Vengurlekar and Inkson.[11]

ACKNOWLEDGMENTS

We thank Dr. H. L. Störmer for discussions. The work at Princeton University is supported by the Office of Naval Research under Contract No. 00014-82-K-0450, the Army Research Office under Contract No. DAAG29-85-K-0098, and a grant from the Siemens Research and Technology Laboratories.

---

*Present address: IBM Thomas J. Watson Research Center, Yorktown Heights, NY 10598.

[1] Pong-Fei Lu, D. C. Tsui, and H. M. Cox, Phys. Rev. Lett. **54**, 1563 (1985).

[2] Y. Katayama and K. Komatsubura, Phys. Rev. Lett. **19**, 1421 (1967).

[3] B. C. Cavenett, Phys. Rev. B **5**, 3049 (1969).

[4] T. W. Hickmott, P. W. Solomon, F. F. Fang, Frank Stern, R. Fischer, and H. Morkoc, Phys. Rev. Lett. **52**, 2053 (1984); *Proceedings of the Seventeenth International Conference on the Physics of Semiconduction, San Francisco, 1984,* edited by D. J. Chadi and W. A. Harrison (Springer-Verlag, New York, 1985), p. 417.

[5] L. Eaves, P. S. S. Guimaraes, B. R. Snell, D. C. Taylor, and K. E. Singer, Phys. Rev. Lett. **55**, 262 (1985); J. Phys. C **18**, L605 (1985).

[6] E. S. Hellman and J. S. Harris, Jr., Bull. Am. Phys. Soc. **30**, 473 (1984); E. S. Hellman, J. S. Harris, C. B. Hanna, and R. B. Laughlin, Physica **134B**, 41 (1985).

[7] C. B. Hanna, E. S. Hellman, and R. B. Laughlin, Phys. Rev. B **34**, 5475 (1986).

[8] J. P. Leburton, Phys. Rev. B **31**, 4080 (1985); Physica **134B**, 32 (1985).

[9] J. Ihm, Phys. Rev. Lett. **55**, 999 (1985).

[10] D. C. Taylor, P. S. S. Guimaraes, F. W. Sheard, B. R. Snell, L. Eaves, G. A. Toombs, and K. E. Singer, Physica **134B**, 12 (1985).

[11] A. S. Vengurlekar and J. C. Inkson, Solid State Commun. **45**, 17 (1983).

[12] H. M. Cox, J. Cryst. Growth **69**, 641 (1984); **73**, 523 (1985).

[13] C. Pickering, J. Electron. Mater. **10**, 901 (1985).

[14] S. Sze, *Physics of Semiconductor Devices,* 2nd ed. (Wiley, New York, 1981).

[15] N. Newman, T. Kendelewicz, L. Bowman, and W. E. Spicer, Appl. Phys. Lett. **46**, 1176 (1985).

[16] R. H. Williams, A. McKinley, G. J. Hughes, and T. P. Humphreys, J. Vac. Sci. Technol. B **2**, 561 (1984).

[17] L. J. Brillson and C. F. Brucker, Surf. Sci. **132**, 212 (1983).

[18] R. H. Williams, R. R. Varma, and A. McKinley, J. Phys. C **9**, 695 (1966).

[19] F. A. Padovani and R. A. Stratton, Solid-State Electron. **9**, 695 (1966).

[20] See, for example, A. G. M. Jansen, A. P. van Gelder, and P. Wyder, J. Phys. C **13**, 6073 (1980).

[21] M. Pepper, J. Phys. C **13**, L717 (1980).

[22] R. Mansfield and I. Ahmasd, J. Phys. C **3**, 423 (1970).

[23] E. W. Fenton and R. R. Haering, Phys. Rev. **159**, 593 (1967).

[24] Y. Yafet, R. W. Keys, and E. N. Adams, J. Phys. Chem. Solids **1**, 137 (1956).

[25] See comments by C. B. Hanna and R. B. Laughlin, and the response by J. Ihm, Phys. Rev. Lett. **56**, 254 (1986).